

initiated either in the upper wall of the chamber or in the counter just above. This picture is unusual, not only because of the size of the shower, but also because of the associated proton that stops in the first lead plate.

The third (Fig. 5c) is a picture of a mesotron shower. This shower differs in its nature from all the others because its particles do not spread out from a central core as the shower progresses, but each particle goes through the second lead plate without multiplying. Most of these par-

ticles are heavier than electrons and several may be specifically identified as mesotrons. It may be noted that there are about four particles in the top of the chamber which seem to converge toward the point where the shower begins. One of these may have been the initiating particle, though the shower may have been started by a non-ionizing particle such as a neutron.

The author wishes to express great appreciation to Dr. Wayne E. Hazen for suggesting the problem and for many very helpful discussions.

The Shape of X-Ray Diffraction Lines from Colloidal Magnesium Oxide

CHESTER RIDLON BERRY*

Cornell University, Ithaca, New York

(Received July 10, 1947)

The broadened diffraction lines from colloidal particles have shapes which depend on the particle size and shape and on the geometrical features of the experiment. An analytical method is developed for eliminating the effect of the geometry of the experiment, thereby giving the shape of the diffraction line. The method is applied to the 200, 220, and 222 lines from colloidal magnesium oxide. The shapes of these diffraction functions in the low intensity regions are not sufficiently accurate to permit the determination of particle shape. The relative half-intensity breadths of curves give best agreement with the values to be expected for cube-shaped particles. The particle size, determined from the Scherrer equation, is 140 angstrom units, and the average deviation from this value is 3.1 percent.

I. INTRODUCTION

MURDOCK¹ gives a theoretical treatment of the breadths and shapes of the x-ray diffraction lines from colloidal powders of the cubic symmetry class. The purpose of the present paper is to give a method for calculating ideal line shapes from experimentally measured line shapes and to apply this method to several diffraction lines. Many investigations have been made on the breadths of broadened diffraction lines, but the shapes of the lines have not been measured because of the difficulty of correcting the measured shape for the effect of experimental conditions.

II. METHOD OF SOLVING FOR THE IDEAL DIFFRACTION FUNCTION

The procedure used in these experiments has been suggested by Jones.² For a given diffraction line a correction curve, $f(y)$, is measured, using a powder containing particles larger than 1000 angstrom units. An uncorrected diffraction curve, $\phi(x)$, is measured, using a colloidal powder of the same material. Jones has shown that these measured functions are related to the ideal diffraction function, $F(y)$, by the integral equation:

$$\phi(x) = \int_{-\infty}^{\infty} f(y) F(x-y) dy = \int_{-\infty}^{\infty} f(x-y) F(y) dy.$$

Knowing the functions $\phi(x)$ and $f(y)$ from experiment, the solution of the equation for $F(y)$

* Present address: Eastman Kodak Company, Research Laboratories, Rochester 4, New York.

¹ C. C. Murdock, work not yet published in full but some of the results are given in *Phys. Rev.* **63**, 223 (1943).

² F. W. Jones, *Proc. Roy. Soc. London* **166**, 16 (1938).

may be accomplished in the following manner. If the Fourier transforms of $\phi(x)$, $f(y)$, and $F(y)$ are, respectively:

$$A(x) = \frac{1}{(2\pi)^{\frac{1}{2}}} \int_{-\infty}^{\infty} \phi(\beta) \exp(-i\beta x) d\beta,$$

$$B(y) = \frac{1}{(2\pi)^{\frac{1}{2}}} \int_{-\infty}^{\infty} f(\beta) \exp(-i\beta y) d\beta,$$

and

$$u(y) = \frac{1}{(2\pi)^{\frac{1}{2}}} \int_{-\infty}^{\infty} F(\beta) \exp(-i\beta y) d\beta,$$

then

$$u(z) = \frac{1}{(2\pi)^{\frac{1}{2}}} \frac{A(z)}{B(z)},$$

and

$$F(y) = \frac{1}{2\pi} \int_{-\infty}^{\infty} \frac{A(z)}{B(z)} \exp(iyz) dz. \quad (1)$$

Since the experimental curves, $\phi(x)$ and $f(y)$, look somewhat like Gaussian distribution curves, they may be approximated rather well by a few terms of a series of Hermitian orthogonal functions,³ the first term of which is the Gaussian distribution. Then let $\phi(x)$ and $f(y)$ be represented as:

$$\phi(x) = \sum_{K=0}^n \gamma_K H_K(x/a) \exp(-x^2/2a^2)$$

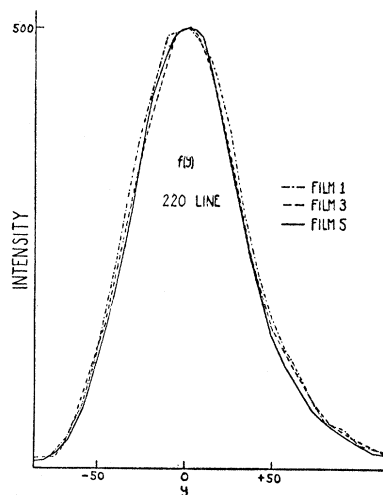


FIG. 1. Correction functions for the 220 reflection from relatively large particles of magnesium oxide.

³ For definitions and some of the properties of Hermitian functions and Hermitian polynomials see: L. Pauling and E. B. Wilson, *Introduction to Quantum Mechanics* (McGraw-Hill Book Company, Inc., New York, 1935), pp. 73-82.

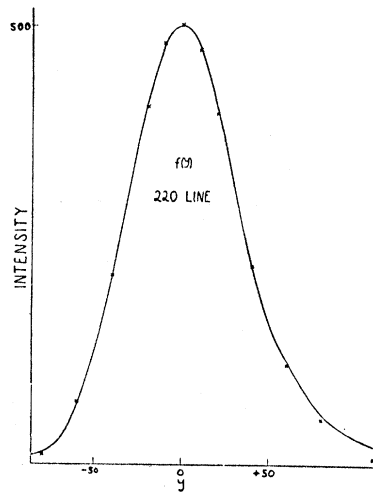


FIG. 2. Average correction function for the 220 magnesium oxide reflection. Crosses show the representation of the correction function by the sum of six terms of a Hermitian expansion.

and

$$f(y) = \sum_{K=0}^n p_K H_K(y/b) \exp(-y^2/2b^2),$$

where a , b , γ_K , and p_K are constants and $H_K(z)$ is the K th order Hermitian polynomial.

The Fourier transforms of $\phi(x)$ and $f(y)$ may then be expressed in the following form:

$$A(z) = a \sum_{K=0}^n \gamma_K (-i)^K H_K(za) \exp(-z^2 a^2/2)$$

and

$$B(z) = b \sum_{K=0}^n p_K (-i)^K H_K(zb) \exp(-z^2 b^2/2).$$

Inserting these expressions in Eq. (1) a relation for $F(y)$ is obtained:

$$F(y) = \frac{1}{2\pi} \frac{a}{b} \int_{-\infty}^{\infty} \frac{\left[\sum_{K=0}^n \gamma_K (-i)^K H_K(za) \right]}{\left[\sum_{K=0}^n p_K (-i)^K H_K(zb) \right]} \times \exp(iyz) \exp(-z^2 a^2/2) \exp(z^2 b^2/2) dz. \quad (2)$$

Inserting the polynomials $H_K(za)$ and $H_K(zb)$ in Eq. (2), the expression in brackets can be simplified, and if higher power terms in z are

neglected, one may write:

$$F(y) = \frac{1}{2\pi} \frac{a}{b} \int_{-\infty}^{\infty} [(l_0 + l_2 z^2 b^2 + \dots + l_{2n} z^{2n} b^{2n}) + i(l_1 z b + l_3 z^3 b^3 + \dots + l_{2n-1} z^{2n-1} b^{2n-1})] \times \exp(iyz) \exp(-z^2 a^2/2) \exp(z^2 b^2/2) dz, \quad (3)$$

where the l 's are constants depending on a , b , γ_K , and ρ_K .

A change of variable from zb to z gives:

$$F(y) = \frac{1}{2\pi} \frac{a}{b} \int_{-\infty}^{\infty} [(l_0 + l_2 z^2 + \dots + l_{2n} z^{2n}) + i(l_1 z + l_3 z^3 + l_{2n-1} z^{2n-1})] \times \exp(iyz/b) \exp(-z^2 a^2/2b^2) \exp(z^2/2) dz. \quad (4)$$

If this change of variable is not made, the coefficients of z in the two sums of Eq. (3) become very large for large powers of z , since b is of the order 30 in the units used for measuring x and y in these experiments. But in Eq. (4) the coefficients become very small for large powers of z .

Then Eq. (4) may be integrated term by term, giving for $F(y)$ an equation of the form:

$$F(y) = \text{constant} \times \exp(-y^2/2a^2 - 2b^2) \times \sum_{K=0}^{2n} C_K (y/b)^K.$$

The constants C_K will decrease rapidly as K increases only if the breadth of the function $f(y)$ at half-maximum intensity is at the most approximately half the breadth of the function $\phi(x)$.

III. EXPERIMENTAL PROCEDURE

To obtain a narrow, intense correction function, $f(y)$, an experimental arrangement was used which gave some focusing of the x-rays at the photographic film. A rocksalt crystal, bent to a radius of 20 cm and ground to a radius of 10 cm, was used as a focusing monochromator.⁴ The $K\alpha$ -radiation reflected from the monochromator was converged to the slit on the circumference of the camera. The x-rays diverged from the slit and fell on the flat powder sample which was

⁴For description of bent rocksalt monochromators see: R. M. Bozorth and F. E. Haworth, Phys. Rev. **53**, 538 (1938).

mounted at the center of the camera. For each diffraction line the surface of the powder was set at the Bragg angle to the ray passing through the center of the camera. Better focusing was obtained by curving the surface of the powder, but the diffraction patterns from flat surfaces could be reproduced more accurately.

Relatively large particles of MgO were obtained by catching the smoke from burning magnesium ribbon. Small particles were obtained by decomposing MgCO_3 in an oven at a temperature of about 640 degrees centigrade.

Sensitometric exposures were made on Eastman Kodak, Type-K, industrial x-ray film for cobalt $K\alpha$ -radiation reflected from a calcite crystal. While maintaining the characteristic $K\alpha$ x-ray intensity constant to within 2.7 percent, exposure times were varied. The densitometer readings were proportional to the time of exposure up to a density of at least 0.60 above chemical fog. In diffraction experiments densities were kept smaller than 0.60 and, assuming no reciprocity failure, were recorded as intensities.

IV. EXPERIMENTAL RESULTS

Figure 1 shows the three determinations of the correction function, $f(y)$, for the 220 line and indicates the accuracy to which measurements were reproduced. At the half-maximum of intensity the average absolute deviation of breadth from the mean value is 2.9 percent. The abscissa unit, y , is a measure of distance on the photographic film and is equal to 1/8000 the angle in

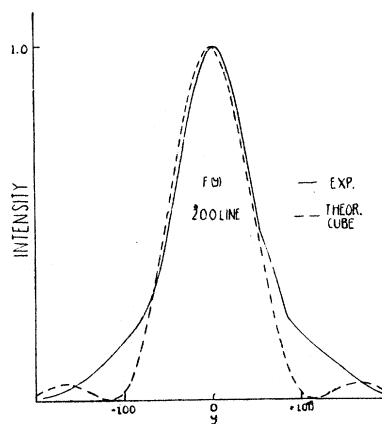


FIG. 3. Corrected diffraction function for the 200 reflection from magnesium oxide and the theoretical diffraction function for cube-shaped particles of uniform size.

radians subtended at the center of the camera. One degree subtended at the center of the camera is very nearly equal to 140 units of y .

Figure 2 shows the curve obtained by taking the average ordinate of the three curves in Fig. 1. The crosses show the representation of $f(y)$ as the sum of the first six terms of a Hermitian expansion. Obviously, greater accuracy in determining line shapes may be obtained by using a larger number of terms in representing the experimental curves, but the computations outlined above become very lengthy. In Fig. 2 the average absolute deviation of the crosses from the experimental curve is 4.3-intensity units, 0.9 percent of the maximum intensity. This was the order of accuracy in representing the various experimental curves by Hermitian sums of six terms.

Figures 3-5, show the plots of the expressions

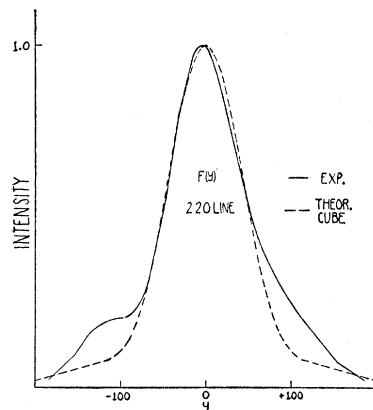


FIG. 4. Corrected diffraction function for the 220 reflection from magnesium oxide and the theoretical diffraction function for cube-shaped particles of uniform size.

for the corrected diffraction functions, $F(y)$, for the 200, 220, and 222 lines, respectively. Plotted in the same figures are the theoretical functions for cube-shaped particles of uniform size. According to Murdock,¹ these functions are

$$F(y) = \sin^2 y / y^2 \text{ for the 200 line,}$$

$$F(y) = 6(y - \sin y) / y^3 \text{ for the 220 line,}$$

and

$$F(y) = 3(y^2 - \sin^2 y) / y^4 \text{ for the 222 line.}$$

Each theoretical function is matched to the corresponding experimental function with respect to breadth at half-maximum intensity. The experimental curves are considerably broader near

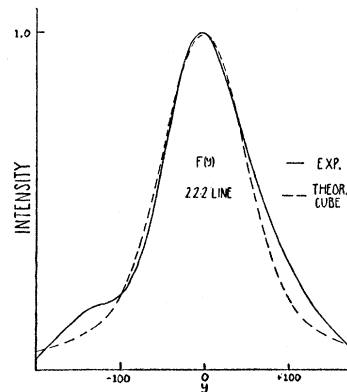


FIG. 5. Corrected diffraction function for the 222 reflection from magnesium oxide and the theoretical diffraction function for cube-shaped particles of uniform size.

the base than the theoretical functions. Moreover, the theoretical functions for particles having tetrahedral, octahedral, rhombic dodecahedral, and spherical shapes lie closer to the theoretical cube function than to the experimental curves.

The irregularities near the position $y = -120$ in the experimental determinations of $F(y)$ for the 220 and 222 lines indicate the inability of the method to produce accurate results in the region of low intensity. The higher order Hermitian coefficients, which are the least accurately known, determine the behavior of $F(y)$ in the region of low intensity. Since the theoretical functions for particles of various shapes differ widely only in the low intensity region, it is not possible to determine the shape of the particles from the shape of the curves shown here.

To check the accuracy of the approximations used in calculating $F(y)$, the second member of the equation

$$\phi(x) = \int_{-\infty}^{\infty} f(x-y)F(y)dy$$

can be evaluated by graphical integration for various values of x and may be compared to the experimentally measured values of $\phi(x)$. Such integrations were performed for each of the diffraction lines at nine values of x . The average absolute deviations of the calculated values of $\phi(x)$ from the measured values were 1.7, 1.4, and 1.3 percent for the 200, 220, and 222 lines, respectively. This error is smaller by a factor of at least two than that obtained when the graphical

integrations of

$$\int_{-\infty}^{\infty} f(x-y)F(y)dy$$

are performed using for $F(y)$ various breadths of theoretical diffraction functions for the different particle shapes. It appears that the excess breadth near the base of the experimental diffraction functions is not an effect introduced by the approximations in solving for $F(y)$. Later discussion will suggest an explanation for this excess breadth.

From the half-maximum intensity breadths of the diffraction functions and the Scherrer equation,⁵ information concerning the size and shape of the particles may be obtained. A form of the Scherrer equation suggested by Murdock⁶ is: $B = K\lambda/V^{1/3} \cos\theta$, where B is the half-maximum intensity breadth of the diffraction line, K is a coefficient depending on the shape of the particles and on the Miller indices of the reflection, θ is the Bragg angle, V is the volume of the particles, and λ is the wave-length of the x-rays. To determine particle size from this equation, the shape must first be known. If the relative breadth of two diffraction lines is calculated, the size of the particles is eliminated, and there remains

$$R = \frac{B_1}{B_2} = \frac{K_1 \cos\theta_2}{K_2 \cos\theta_1}$$

B_1/B_2 can be evaluated from the experimental curves and may be compared with the values obtained from the right member of the equation when the values of K corresponding to the various particle shapes are inserted. The relative

TABLE I. Ratios of the observed relative breadths to the theoretical relative breadths of the diffraction lines for particles of various shapes.

Form—	Tetra- hedron	Octa- hedron	Dodeca- hedron	Sphere	Cube
$\frac{R_{200/220}}{R_{200/200}}$ observed	0.820	1.220	1.170	1.155	1.090
$\frac{R_{200/220}}{R_{200/200}}$ theoretical					
$\frac{R_{222/200}}{R_{222/200}}$ observed	1.050	0.790	0.870	0.905	0.940
$\frac{R_{222/200}}{R_{222/200}}$ theoretical					
$\frac{R_{222/220}}{R_{222/220}}$ observed	0.855	0.965	1.005	1.050	1.020
$\frac{R_{222/220}}{R_{222/220}}$ theoretical					

⁵ P. Scherrer, Göttinger Nachrichten 2, 98 (1918).

⁶ C. C. Murdock, Phys. Rev. 35, 8 (1930).

breadths of the experimentally measured diffraction functions are $B_{200}/B_{220} = 0.993$, $B_{222}/B_{200} = 1.244$, and $B_{222}/B_{220} = 1.236$. The ratios of the observed relative breadths to the theoretical relative breadths for particles of various shapes are given in Table I.

From Table I the shape which gives the best approximation to the value 1.000 is the cube. The average absolute deviation for the various shapes from the value 1.000 is 0.057 for the cube, 0.100 for the sphere, 0.102 for the dodecahedron, 0.125 for the tetrahedron, and 0.155 for the octahedron.

Assuming the particles are cubes, the mean size can be found from the Scherrer equation. The measured half-maximum intensity breadths of the three calculated diffraction functions are: $B_{200} = 1.27 \times 10^{-2}$ radian, $B_{220} = 1.28 \times 10^{-2}$ radian, and $B_{222} = 1.59 \times 10^{-2}$ radian. Then the cube root of the volume of the particles as calculated from these line breadths is 134, 145, and 142 angstroms, respectively. This gives a mean value of 140 angstroms and an average absolute deviation from the mean of 3.1 percent.

If the size of the particles were calculated assuming a spherical shape, the cube root of the volume would be 134, 154, and 147 angstroms for the 200, 220, and 222 lines, respectively. This gives a mean value of 145 angstroms and an average deviation from the mean of 5.1 percent.

Electron micrographs of the magnesium oxide powder were made by Dr. James Hillier of the RCA Laboratory. The size of the particles appears two to three times larger in linear dimension than the above values. It seems likely that aggregates and not single crystals appear in the micrographs. The shape of the particles cannot readily be determined, but it does not appear that they are regular cubes in aggregates, except in a few instances.

A study was made of the effect on the diffraction function of a distribution of particle sizes. The theoretical calculations by Murdock¹ give the diffraction functions for the case of particles of uniform size. If $F(a_m y)$ is the theoretical diffraction function for particles of a given size, the resultant diffraction function for a discrete distribution of sizes will be

$$F(y) = \sum_m W_m F(a_m y) / \sum_m W_m,$$

where W_m is a weighting factor which depends on the particle size. W_m is proportional to the number of particles, N_m , of a given size, to the intensity, I_m , diffracted by a single particle of a given size, and inversely proportional to the area, A_m , of the diffraction function for particles of a given size. I_m is very nearly proportional to the volume of the crystal. It can be seen from the Scherrer equation and the theoretical diffraction functions that A_m is inversely proportional to the cube root of the volume of the crystals. Then the weighting factor is $W_m = CN_m V_m^{4/3}$. The resultant diffraction function due to a mixture of sizes will then be

$$F(y) = \frac{\sum_m N_m V_m^{4/3} F(a_m y)}{\sum_m N_m V_m^{4/3}}.$$

The half-maximum intensity breadth of this function will give the observed mean size of the particles. Since the diffraction function is weighted in favor of the larger particles, the measured mean size will be expected to be too large in practice. The effect on the diffraction function of various distributions of particle size was investigated using the above relation. A

discrete distribution of particle sizes, approximating the continuous Gaussian distribution, does not seem to change the shape of the diffraction function appreciably. However, a distribution in which there are a large number of relatively small particles gives a diffraction function which is broad near the base. For example, the calculation was made for the 220 reflection from cube-shaped particles when there are four times as many particles of 75 angstrom edge length as of 150 angstrom edge length. The half-intensity breadth gave a mean edge length of 135 angstrom units, but the resultant line shape corresponded to the shape for cubes of uniform size only in the upper half. In the lower half the resultant function was much broader than the function for cubes of uniform size. It seems reasonable that some such distribution of particle sizes may account for the experimentally determined diffraction functions.

The author wishes to thank Professor Carleton C. Murdock, who suggested the problem, for his encouragement and assistance in carrying out the research.

On the Dissociation Energy of Carbon Monoxide and the Heat of Sublimation of Carbon

HOMER D. HAGSTRUM

Bell Telephone Laboratories, Murray Hill, New Jersey

(Received June 26, 1947)

None of the values of the dissociation energy of carbon monoxide, $D(\text{CO})$, proposed on the basis of interpretations of predissociations in the spectrum of CO is in satisfactory agreement with the results of electron-impact experiments. The only possible interpretation of these experiments gives $D(\text{CO}) = 9.6$ ev. Compelling reasons can be given for considering this result of sufficient accuracy to make it irreconcilable with any of the values from the band spectrum. A new interpretation of the effects in the spectrum which brings agreement with the electron impact value is possible, however. It involves a potential curve with maximum for $J=0$ for the state $a' \ ^3\Sigma^+$ of CO which predissociates $B^1\Sigma^+$ and $b^3\Sigma^+$ at 11.11 ev. Various data favor this interpretation and its consequences. Satisfactory agreement among all data bearing on $D(\text{CO})$ and $L_1(\text{C})$, the heat of sublimation of carbon, can be attained in this way.

1. INTRODUCTION

THE dissociation energy of carbon monoxide, $D(\text{CO})$, is a particularly important quantity because of its relation to the heat of sublima-

tion of carbon, $L_1(\text{C})$, and through it to the heats of formation and bond energies of every carbon-containing molecule. The relation between $L_1(\text{C})$ and $D(\text{CO})$ is obtained from the well-known